Journal of Engineering Physics and Thermophysics, Vol. 82, No. 4, 2009

INFLUENCE OF TWO-DIMENSIONAL CONVECTION ON SOLIDIFICATION OF BACK-TAPERED INGOTS

V. V. Dremov

UDC 539.19

The influence of two-dimensional convection on the rate of solidification of a flat-shaped ingot in a wedge mold has been studied theoretically. The appearance of three crystalline zones in a solidified ingot is explained.

Keywords: *solidified front, convection, flat-shaped mold, liquid and solid phases, superheating heat, variational method, stationary case, nonstationary solution, solidification curves, structure zones.*

Introduction. Solidification of a metal in a straight-tapered mold was calculated theoretically in [1], and with a more accurate allowance for the influence of convection in [2]. In the present work, the problem of the influence of convection on solidification of back-tapered ingots is investigated.

Statement of the Problem. Taking into account the fact that the rate at the solidified front and on the metal surface, as a result of it being covered with slag, is equal to zero and convection can develop as a vortex filling half the mold with a maximum velocity value $v_{\max}$ in the central region of the liquid phase at the beginning of solidification and based on the results of [2], we obtain

$$v_r = \frac{4v_{r\max}}{(R_2 - R_1)^2}(r - R_1)(r_f - r)\cos\left(\frac{\varphi}{\varphi_f}\pi\right). \tag{1}$$

The two-dimensional continuity equation in the cylindrical coordinate system will be written as

$$\frac{\partial}{\partial r}(rv_r) = -\frac{\partial v_\varphi}{\partial \varphi}. \tag{2}$$

Substituting Eq. (1) into this equation, we obtain

$$v_\varphi = -\frac{4v_{r\max}}{(R_2 - R_1)^2}\left(2R_1 r - 3r^2 - R_1 r_f + 2rr_f\right)\frac{\varphi_f}{\pi}\sin\left(\frac{\varphi}{\varphi_f}\pi\right). \tag{3}$$

Considering solidification of a metal in a flat-shaped mold in the statement of [1], we write the system of equations of heat conduction in the liquid and solid phases in the cylindrical coordinate system in the form

$$\frac{\partial T_1}{\partial t} + v_r\frac{\partial T_1}{\partial r} + \frac{v_\varphi}{r}\frac{\partial T_1}{\partial r} = a_1\left[\frac{1}{r}\frac{\partial}{\partial r}\left(r\frac{\partial T_1}{\partial r}\right) + \frac{1}{r^2}\frac{\partial^2 T_1}{\partial \varphi^2}\right], \tag{4}$$

Here $0 < \varphi < \varphi_f$, $R_1 < r < r_f$;

$$\frac{\partial T_2}{\partial t} = a_2\left[\frac{1}{r}\frac{\partial}{\partial r}\left(r\frac{\partial T_2}{\partial r}\right) + \frac{1}{r^2}\frac{\partial^2 T_2}{\partial \varphi^2}\right] \tag{5}$$

Donbass National Academy of Civil Engineering and Architecture, 2 Derzhavin Str., Makeevka, Donetsk District, 86123, Ukraine. Translated from Inzhenerno-Fizicheskii Zhurnal, Vol. 82, No. 4, pp. 711–717, July–August, 2009. Original article submitted April 4, 2008; revision submitted December 8, 2008.

for the region with $\varphi_f < \varphi < \alpha$, $r_f < r < R_2$.

The thickness of the solidified crust for any radius is determined from the equation

$$\varepsilon (r_f, \varphi_f, t_f) = r_f (t_f) [\alpha - \varphi_f (t_f)] . \quad (6)$$

It is considered that the chord coincides with an arc at small arc length; this corresponds to a small angle α. At time $t = 0$ the solid phase is absent, and the temperature of the liquid metal poured into the mold $T_1(r, \varphi, 0) = T_{in}$ for $R_2 > r > R_1$ and $\alpha > \varphi > 0$. At $\varphi = \alpha$, $r = R_2$, and $t > 0$ the process of solidification begins and

$$T_1 (r_f, \varphi_f, t_f) = T_{cr} , \quad (7)$$

$$T_2 (r, \alpha, t) = T_s . \quad (8)$$

The thermal contact at the solidified front is considered perfect; therefore at $r = r_f(t)$ and $\varphi = \varphi_f(t)$ the temperatures of the liquid and solid phases are equal to the solidification temperature:

$$T_1 (r_f, \varphi_f, t_f) = T_2 (r_f, \varphi_f, t_f) = T_{cr} . \quad (9)$$

Moreover, on the moving phase transition front, latent heat of solidification L_1 is released that is transferred through the solid phase together with the superheating heat:

$$\lambda_1 \left(\frac{1}{r} \frac{\partial T_1}{\partial \varphi} \right)_f + L_1 \rho \frac{\partial \varepsilon}{\partial t} = \lambda_2 \left(\frac{1}{r} \frac{\partial T_2}{\partial \varphi} \right)_f . \quad (10)$$

Condition (10) has been written on the assumption that the mold height is much larger than its width, and the heat flux through the bottom and ceiling of the mold can be neglected. Equation (10) allows one to determine the dependence of the thickness of the solid crust on time $\varepsilon(t)$. From Eqs. (4)–(6) and boundary conditions (7)–(10) one has to find three unknown functions $T_1(r, \varphi, t)$, $T_2(r, \varphi, t)$, and $\varepsilon(t)$.

Solution of the Problem. A stationary approximate solution of the equation over r will be presented in a form similar to that given in [1]:

$$T_1 = T_{in} - \frac{r - R_1}{r_f - R_1} (T_{in} - T_{cr}) . \quad (11)$$

An approximate solution of Eq. (4) is sought by the variational method [3], with gradual complication of the problem. First, we will find the dependence over φ for the stationary case:

$$v_r \frac{\partial T_1}{\partial r} + \frac{v_\varphi}{r} \frac{\partial T_1}{\partial \varphi} = a_1 \left[\frac{1}{r} \frac{\partial}{\partial r} \left(r \frac{\partial T_1}{\partial r} \right) + \frac{1}{r^2} \frac{\partial^2 T_1}{\partial \varphi^2} \right] . \quad (12)$$

Omitting the subscript 1 at the temperature, designating the derivatives as $T_r = \partial T/\partial r$, $T_{\varphi\varphi} = \partial^2 T/\partial \varphi^2$, $T_{rr} = \partial^2 T/\partial r^2$, and multiplying Eq. (12) by r, we obtain

$$\frac{v_r}{a_1} r T_r + \frac{v_\varphi}{a_1} T_\varphi - T_r - r T_{rr} - \frac{1}{r} T_{\varphi\varphi} = 0 . \quad (13)$$

The functional corresponding to Eq. (13) will be written in the form

$$\int_{r_f}^{R_1} \int_0^{\varphi_f} \left[2 \frac{v_r}{a_1} r T_r^0 T + 2 \frac{v_\varphi}{a} T_\varphi^0 T + r T_r^2 + \frac{1}{r} T_\varphi^2 \right] dr d\varphi = L . \quad (14)$$

We seek a function that minimizes functional (14) in the form

$$T = T(r) f(\varphi) = \left[T_{\text{in}} - \frac{r - R_1}{r_{\text{f}} - R_1} (T_{\text{in}} - T_{\text{cr}}) \right] f(\varphi) . \tag{15}$$

Computing the derivatives with respect to r and φ from (15), we obtain

$$T_r = -\frac{T_{\text{in}} - T_{\text{cr}}}{r_{\text{f}} - R_1} f(\varphi) , \quad T_\varphi = \left[T_{\text{in}} - \frac{r - R_1}{r_{\text{f}} - R_1} (T_{\text{in}} - T_{\text{cr}}) \right] f'(\varphi) . \tag{16}$$

Substituting (15) and (16) into Eq. (14) and integrating over r, we find

$$\int_0^{\varphi_{\text{f}}} \left\{ A_1 f^0 f + B_1 (f_\varphi)^0 f + C_1 f^2 + D_1 (f_\varphi)^2 \right\} d\varphi = L . \tag{17}$$

The function $f(\varphi)$ is selected so that the integral in Eq. (17) is minimal. This condition is satisfied by a function that makes the variation of the functional vanish, $\delta L = 0$, which corresponds to the fulfillment of the Euler–Lagrange equation:

$$\frac{\partial L}{\partial f(\varphi)} - \frac{\partial}{\partial \varphi} \frac{\partial L}{\partial f'(\varphi)} = 0 . \tag{18}$$

Taking derivatives of (17) and substituting them into Eq. (18), we obtain

$$f''(\varphi) - \frac{A}{k} \sin(k\varphi) f'(\varphi) - \left[B + \frac{A}{2} \cos(k\varphi) \right] f(\varphi) = 0 , \tag{19}$$

where $A = B_1/(2D_1)$; $B = C_1/D_1$; $k = \pi/\varphi_{\text{f}}$. The solution of Eq. (19) will be sought in the form of the function

$$f(\varphi) = a(\varphi) (C_1 \cosh \omega\varphi + C_2 \sinh \omega\varphi) , \tag{20}$$

where $a(\varphi)$ is the unknown function φ and ω is a constant independent of φ.

Substituting Eq. (20) into (19) and writing out the coefficients at cosh (ωφ) and sinh (ωφ), we obtain two identical differential equations for the function α(φ) with the constants C_1 and C_2. Since these constants are independent, we will write one of the equations for C_1 in the form

$$a'' - \left(\frac{A}{k} \sin k\varphi \right) a' - \left(B + \frac{A}{2} \cos k\varphi - \omega^2 \right) a = 0 , \tag{21}$$

and for C_2 in the form

$$2a' - a \frac{A}{k} \sin k\varphi = 0 . \tag{22}$$

Solving Eq. (22), we obtain

$$a = \exp\left(-\frac{A}{2k^2} \cos k\varphi \right). \tag{23}$$

Substituting Eq. (23) into Eq. (22), we find

$$\omega = \sqrt{B + \frac{A^2}{4k^2} \sin^2 k\varphi} \ , \tag{24}$$

where ω is the function of φ. To satisfy the initial condition, we assume that the function $\sin^2 k\varphi$ is equal to an average value, i.e., 1/2. Therefore finally we have

$$\omega = \sqrt{B + \frac{A^2}{8k^2}} \ , \tag{25}$$

$$f(\varphi) = \exp\left(-\frac{A}{2k^2} \cos k\varphi\right)(C_1 \cosh \omega\varphi_f + C_2 \sinh \omega\varphi_f) \ . \tag{26}$$

The constants C_1 and C_2 will be found from the boundary conditions: $T = T_{cr}$ at $\varphi = \varphi_f$ and $\partial T/\partial\varphi = 0$ at $\varphi = 0$. Substituting (26) into (15) and taking into account that $\varphi = \varphi_f$ and $r = r_f$, we obtain

$$1 = \exp\left(\frac{A}{2k^2}\right)(C_1 \cosh \omega\varphi_f + C_2 \sinh \omega\varphi_f) \ . \tag{27}$$

Having evaluated the derivative with respect to φ of Eq. (15) with the substituted function (26) and with account for the fact that φ = 0, we find

$$\left[T_{in} - \frac{r - R_1}{r_f - R_1}(T_{in} - T_{cr})\right] C_2 \omega \exp\left(-\frac{A}{2k^2}\right) = 0 \ , \tag{28}$$

whence it follows that $C_2 = 0$ and C_1 is determined from Eq. (27). The complete solution of Eq. (19) has the form

$$T_1 = \left[T_{in} - \frac{r - R_1}{r_f - R_1}(T_{in} - T_{cr})\right] \exp\left[-\frac{A}{2k^2}(1 + \cos k\varphi)\right] \frac{\cosh \omega\varphi}{\cosh \omega\varphi_f} \ . \tag{29}$$

In the solution obtained the dependence on φ is more complex than in [1] and differs from it by the presence of the preexponential factor that more accurately allows for the influence of convection in the field of liquid metal.

To find a complete nonstationary solution of the heat conduction equation (4), we will write the functional corresponding to this equation:

$$L = \int_0^{t_f} \int_0^{\varphi_f} \int_{r_f}^{R_1} \left[2 \frac{v_r}{a_1} r T_r^0 T + 2 \frac{v_\varphi}{a} T_\varphi^0 T + 2 \frac{r}{a_1} T T_t^0 + r T_r^2 + \frac{1}{r} T_\varphi^2\right] dt dr d\varphi \ . \tag{30}$$

The solution of Eq. (30) is sought in the form of the function (29) multiplied by the unknown function $f(t)$:

$$T_1 = \left[T_{in} - \frac{r - R_1}{r_f - R_1}(T_{in} - T_{cr})\right] \frac{\cosh \omega\varphi}{\cosh \omega\varphi_f} \exp\left[-\frac{A}{2k^2}(1 + \cos k\varphi)\right] f(t) \ . \tag{31}$$

The substitution of Eq. (31) into (30) and integration over r and φ yield

$$L = \int_0^{t_f} \left\{K f^0(t) f(t) + M f(t) [f'(t)]^0 + P f^2(t) + S f^0(t) f(t) + Q f^2(t)\right\} dt \ . \tag{32}$$

Varying (32) over $f(t)$ and equating the variation to zero, we obtain

$$Mf'(t) + G_1 f(t) = 0\,, \quad G_1 = K + S + 2\,(P + Q)\,. \tag{33}$$

The following function will be the solution of Eq. (33):

$$f(t) = C \exp\,(-\,G_1 t/M)\,. \tag{34}$$

The constant C will be found from the condition at the crystallization front:

$$T_1\,(r = r_{\rm f}\,,\ \varphi = \varphi_{\rm f}\,,\ t = t_{\rm f}) = T_{\rm cr}\,. \tag{35}$$

For this purpose, we will write the solution of the nonstationary problem following for (34) in (31). As a result, we obtain

$$T_1 = \left[T_{\rm in} - \frac{r - R_1}{r_{\rm f} - R_1}\,(T_{\rm in} - T_{\rm cr})\right] \frac{\cosh\,\omega\varphi}{\cosh\,\omega\varphi_{\rm f}} \exp\left[-\frac{A}{2k^2}\,(1 + \cos\,k\varphi)\right] C \exp\left(-\frac{G_1}{M}\,t\right). \tag{36}$$

The substitution of Eq. (36) into Eq. (35) yields $C = \exp\,(G_1 t_{\rm f}/M)$. Thus the following function is the solution of Eq. (4):

$$T_1 = \left[T_{\rm in} - \frac{r - R_1}{r_{\rm f} - R_1}\,(T_{\rm in} - T_{\rm cr})\right] \frac{\cosh\,\omega\varphi}{\cosh\,\omega\varphi_{\rm f}} \exp\left[-\frac{A}{2k^2}\,(1 + \cos\,k\varphi) - \frac{G_1}{M}\,(t - t_{\rm f})\right]. \tag{37}$$

It should be noted that the difference $(t - t_{\rm f})$ is always positive, and it determines the interval of time during which the crystallization front attains the value of the coordinates (r, φ) when $t_{\rm f}$ is taken as the coordinate origin.

The solution of Eq. (5) will be found likewise:

$$T_2 = \left[T_{\rm cr} - \frac{r - r_{\rm f}}{R_2 - r_{\rm f}}\,(T_{\rm cr} - T_{\rm s})\right] \frac{\sinh\left[(\alpha - \varphi)\sqrt{\dfrac{A_2}{B_2}}\right] + \sinh\left[(\varphi - \varphi_{\rm f})\sqrt{\dfrac{A_2}{B_2}}\right]}{\sinh\left[(\alpha - \varphi)\sqrt{\dfrac{A_2}{B_2}}\right]} \exp\left[-\frac{2G_2\,(t - t_{\rm f})}{F_2}\right], \tag{38}$$

where

$$A_2 = \frac{(r_{\rm f} + R_2)\,(T_{\rm cr} - T_{\rm s})^2}{2\,(R_2 - r_{\rm f})}\,; \tag{39}$$

$$B_2 = T_{\rm cr}^2 \ln\frac{R_2}{r_{\rm f}} - 2T_{\rm cr}\,(T_{\rm cr} - T_{\rm s})\left(1 - \frac{r_{\rm f}}{R_2 - r_{\rm f}} \ln\frac{R_2}{r_{\rm f}}\right) + (T_{\rm cr} - T_{\rm s})^2 \left[\frac{r_{\rm f}^2 \ln\dfrac{R_2}{r_{\rm f}}}{(R_1 - r_{\rm f})^2} - \frac{3r_{\rm f} - R_2}{2\,(R_2 - r_{\rm f})}\right]. \tag{40}$$

Calculating the derivatives with respect to φ of Eqs. (37) and (38) with account for the fact that at the solidified front $r = r_{\rm f}$, $\varphi = \varphi_{\rm f}$, and $t = t_{\rm f}$ and substituting them into Eq. (10), we find

$$r_{\rm f} \frac{dr_{\rm f}}{dt}\,(\alpha - \varphi_{\rm f}) = \frac{T_{\rm cr}}{L_1 \rho} \left\{\lambda_2 \sqrt{\frac{A_2}{B_2}}\, \frac{\cosh\left[(\alpha - \varphi_{\rm f})\sqrt{\dfrac{A_2}{B_2}}\right] - 1}{\sinh\left[(\alpha - \varphi_{\rm f})\sqrt{\dfrac{A_2}{B_2}}\right]} + \lambda_1 \omega \tanh\,\omega\varphi_{\rm f}\right\}. \tag{41}$$

The coefficients needed for the calculation of ω from Eq. (25) with allowance for the designations for Eq. (19), are as follows:

$$B_1 = \frac{4}{3}\frac{v_{r\max}\,(T_{\text{in}} - T_{\text{cr}})}{a_1\,(R_2 - R_1)^2\,(r_{\text{f}} - R_1)}$$

$$\times\left[T_{\text{in}}\left(R_1^4 - 2r_{\text{f}}R_1^3 + 2R_1 r_{\text{f}}^3 - r_{\text{f}}^4\right) - \frac{T_{\text{in}} - T_{\text{cr}}}{5\,(r_{\text{f}} - R_1)}\left(-2R_1^5 + 5R_1^4 r_{\text{f}} - 10R_1^2 r_{\text{f}}^3 + 10R_1 r_{\text{f}}^4 - 3r_{\text{f}}^5\right)\right],$$

$$D_1 = T_{\text{in}}^2 \ln\frac{r_{\text{f}}}{R_1} - 2T_{\text{in}}\,(T_{\text{in}} - T_{\text{cr}})\left(1 - \frac{R_1}{r_{\text{f}} - R_1}\ln\frac{r_{\text{f}}}{R_1}\right) + (T_{\text{in}} - T_{\text{cr}})^2\left[\frac{R_1^2 \ln\dfrac{r_{\text{f}}}{R_1}}{(r_{\text{f}} - R_1)^2} - \frac{3R_1 - r_{\text{f}}}{2\,(r_{\text{f}} - R_1)}\right],$$

$$C_1 = \frac{r_{\text{f}} + R_1}{2\,(r_{\text{f}} - R_1)}\,(T_{\text{in}} - T_{\text{cr}})^2 . \tag{42}$$

Integrating Eq. (41), we find

$$r_{\text{f}}^2 = R_2^2 - \frac{2T_{\text{cr}}C_*}{L_1\rho\,(\alpha - \varphi_{\text{f}})}\,t_{\text{f}}\,, \tag{43}$$

where C_* is the expression in braces in Eq. (41). The minus sign appears because in a back-tapered mold the radial coordinate of the solidified front decreases with increases in time. If we calculate the time in which the solidified front reaches the coordinate r_{f} with φ_{f} fixed, we will obtain the equation

$$t_{\text{f}} = \frac{L_1\rho\,(\alpha - \varphi_{\text{f}})}{2T_{\text{cr}}C_*}\left(R_2^2 - r_{\text{f}}^2\right). \tag{44}$$

Discussion of Results. Using Eq. (44), numerical calculations were carried out, and graphs of the function $t_{\text{f}}(\varphi_{\text{f}})$ were constructed for different coordinates r_{f} at the following numerical values of the dimensions of a mold and parameters of liquid and solid steel: R_1 = 1.2 m, R_2 = 2.2 m, $\alpha = 10^{\text{o}}$, T_{in} = 1783 K, T_{cr} = 1733 K, T_{s} = 233 K, $a_1 = 4.5\cdot10^{-6}$ m^2/sec, λ_1 = 26.5 W/(m·K), λ_2 = 30.3 W/(m·K), $\rho = 7.31\cdot10^3$ kg/m^3, and $L_1 = 2.72\cdot10^5$ J/kg. Figure 1 presents the graphs for $t_{\text{f}}(\varphi_{\text{f}}, r_{\text{f}})$ with $v_r = 10^{-1}$, $5\cdot10^{-2}$, $\cdot10^{-2}$, and $\cdot10^{-3}$ m/sec. In the graphs there are three zones corresponding to different velocities of the solidified front, which are illustrated by different slopes of the curves. For example, for r_{f} = 1.6 m the first zone is located from φ_{f} = 0.17 rad to φ_{f} = 0.1 rad, which corresponds to the times from zero to $6\cdot10^2$ sec and the average velocity of the solidified front is equal to ~0.22 mm/sec. The second zone lies within the range from φ_{f} = 0.1 rad to φ_{f} = 0.02 rad and corresponds to the times from $t_{\text{f}} = 6\cdot10^2$ sec to $t_{\text{f}} = 4.5\cdot10^3$ sec, whence it follows that v_{f2} = 0.04 mm/sec. The third zone lies within the range from φ_{f} = 0.02 to φ_{f} = 0, and in the time interval from $t_{\text{f}} = 4.5\cdot10^3$ sec to $t_{\text{f}} = 4.9\cdot10^3$ sec, whence it follows that v_{f3} = 0.08 mm/sec.

Conclusions. Thus, in the beginning solidification proceeds at a high rate in the 1st zone, then slows down in the 2nd, and is accelerated again in the 3rd. Such a behavior of the solidified front may explain the presence of the three zones formed in a solidified ingot: first, which corresponds to the 1st zone, a fine-crystal structure is formed; then, in the 2nd zone, columnar crystals are formed, then equiaxial crystals in the 3rd zone. As the velocity of convection decrease, the 1st and 2nd zones become smaller and the 3rd zone of equiaxial crystals extends. This is especially evident in Fig. 1c and d for $v_r = 10^{-2}$ and 10^{-3} m/sec.

A comparison of the results of the theory with experiments carried out in [4, 5] shows that the solidification rate in the second zone up to the moment of the beginning of accelerated solidification (in the terminology of the authors of those works) atlains a value equal to 3 mm/min or 0.05 mm/sec (according to the graph given in [5] on page 65). As is seen from the foregoing calculations, the velocity of motion of the solidified front in the second zone amounts to v_{f} = 0.04 mm/sec.

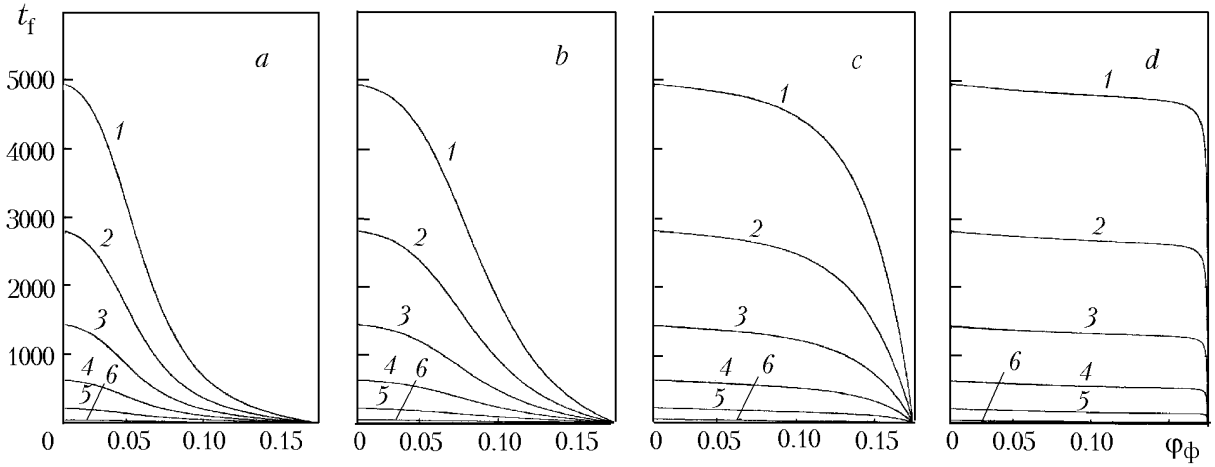

Fig. 1. Motion of the solidified front $t_f(\varphi_f)$ at different convection velocities v_r (a) 10^{-1} m/sec; b) $5 \cdot 10^{-2}$; c) 10^{-2}; d) 10^{-3}): 1) r_f = 1.6 m; 2) 1.7; 3) 1.8; 4) 1.9; 5) 2.0; 6) 2.1. t_f, sec; φ_f, rad.

One other comparison of the obtained theoretical values of the solidification rate with the experimental data presented in [6] in Fig. 243 as a graph for different crystalline zones shows that corresponding to the 1st zone of fine-crystalline crystals in the graph are the solidified front motion velocities above 0.17 mm/sec, corresponding to the 2nd zone of columnar crystals are the velocities from 0.134 to 0.067 mm/sec, and in the 3rd zone of equiaxial crystals — from 0.067 to 0.02 mm/sec and from 0.02 to 0.07 mm/sec. It is seen that the solidified front motion velocities in the 1st and 3rd zones approximately coincide with theoretical ones but differ from those observed in the 2nd zone. In [6] the parabola of the dependence of velocities on coordinates has a minimum in the 3rd zone, whereas in the theoretical calculations it lies in the 2nd zone, but this is for r_f = 1.6 m. For other values of r_f and convection velocities the results will be different, and they can be calculated from the graphs given. An ingot in the experiment weighed 13 tons and in the theoretical calculation it was of 5 tons in weight. The values of convection velocities in the experiment are not given. The side wall thickness in the theoretical calculation was equal to 1.6 sin 10^0 = 0.28 m, whereas the experimental curve is given for a thickness of 0.36 m.

The accelerated vertical solidification found by the authors of [4] is correctly explained by them thus: "at this moment, linking of the boundaries of the solid phase moving from the side walls of the mold occurs." Therefore the velocity of covering of the crater by the moving side solidified fronts cannot be considered to be the rate of vertical solidification, i.e., the motion of the horizontal front in the vertical direction, and the square root law derived for the motion of fronts is not rejected by the given law.

NOTATION

A_1, B_2, C_1, D_1, A_2, B_2, constants of integration over radius; a_1, a_2, thermal diffusivities of liquid and solid metal, m^2/sec; K, M, P, S, Q, constants of integration over r and φ; L_1, crystallization heat, J/kg; L, functional or Lagrangian; R_1, R_2, lower and upper radii of the mold, m; r, φ, cylindrical coordinates of points inside the mold; T_1, temperature of a liquid metal inside the mold, K; T_2, temperature of solid metal inside the load, K; T_{cr}, crystallization temperature, K; T_s, temperature of the bottom and side surface of the mold, K; T_{in}, initial temperature of casting, K; T_r^0, T_φ^0, T_t^0, unvaried derivatives with respect to temperature over the radius, angle, and time; T, temperature function; T_r, T_{rr}, T_φ, $T_{\varphi\varphi}$, T_t, first and second derivatives over radius, angle, and time; t, time, sec; t_f, time at crystallization front, sec; v_r, v_φ, radial and azimuthal velocity components in the mold, m/sec; α, angle of taper of the side walls of the mold; ε, thickness of solidified metal in a mold, m; λ_1, λ_2, thermal conductivities of a liquid and solid metal, W/(m·K); ρ_1, ρ_2, densities of liquid and solid metal, kg/m^3; ρ, average density of the metal, kg/m^3; φ_f, r_f, azimuthal and radial coordinates of the point at the solidification front in a mold. Subscripts: cr, crystallization; in, initial; s, mold surface; f, front; m, maximal.

REFERENCES

1. V. V. Dremov and F. V. Nedopekin, Analytical calculation of solidification of a melt in a mold, *Inzh.-Fiz. Zh.*, **75**, No. 6, 179–184 (2002).
2. V. V. Dremov, Solidification of a melt in a mold in the presence of convective flows, in: *Proc. 14th Int. Conf. on Metallurgical Heat Engineering*, Dnepropetrovsk (2005), pp. 198–207.
3. R. S. Schechter, *The Variational Method in Engineering* [Russian translation], Mir, Moscow (1971), p. 110.
4. E. A. Kazachkov, Solidification and inhomogeneity of large sheet ingots, in: *Problems of the Theory and Practice of Steel-Smelting Production* [in Russian], Metallurgiya, Moscow (1991), pp. 154–166.
5. Yu. A. Samoilovich, V. I. Timoshpol'skii, I. A. Trusova, and V. V. Filimonov, *Steel Ingot* [in Russian], Vol. 2, Belorusskaya Nauka, Minsk (2000), p. 65.
6. V. A. Efimov, *Casting and Crystallization of Steel* [in Russian], Metallurgiya, Moscow (1976), p. 314.